C–C bond formation by cyanide addition to dinuclear vinyliminium complexes

Vincenzo G. Albano [b], Luigi Busetto [a], Fabio Marchetti [a], Magda Monari [b], Stefano Zacchini [a], Valerio Zanotti [a,*]

[a] *Dipartimento di Chimica Fisica e Inorganica, Università di Bologna, Viale Risorgimento 4, 40136 Bologna, Italy*
[b] *Dipartimento di Chimica "G. Ciamician", Università di Bologna, Via Selmi 2, 40126 Bologna, Italy*

Abstract

The diiron vinyliminium complexes $[Fe_2\{\mu-\eta^1:\eta^3-C(R')=C(H)C=N(Me)(R)\}(\mu-CO)(CO)(Cp)_2][SO_3CF_3]$ (R = Me, R′ = SiMe_3 (**1a**); R = Me, R′ = CH_2OH (**1b**); R = CH_2Ph, R′ = Tol (**1c**), Tol = 4-MeC_6H_4; R = CH_2Ph, R′ = COOMe (**1d**); R = CH_2Ph, R′ = SiMe_3 (**1e**)) undergo regio- and stereo-selective addition by cyanide ion (from NBu$_4^n$CN), affording the corresponding bridging cyano-functionalized allylidene compounds $[Fe_2\{\mu-\eta^1:\eta^3-C(R')C(H)C(CN)N(Me)(R)\}(\mu-CO)(CO)(Cp)_2]$ (**3a–e**), in good yields. Similarly, the diiron vinyliminium complexes $[Fe_2\{\mu-\eta^1:\eta^3-C(R')=C(R')C=N(Me)(R)\}(\mu-CO)(CO)(Cp)_2][SO_3CF_3]$ (R = R′ = Me (**2a**); R = Me, R′ = Ph (**2b**); R = CH_2Ph, R′ = Me (**2c**); R = CH_2Ph, R′ = COOMe (**2d**)) react with cyanide and yield $[Fe_2\{\mu-\eta^1:\eta^3-C(R')C(R')C(CN)N(Me)(R)\}(\mu-CO)(CO)(Cp)_2]$ (**9a–d**). The reactions of the vinyliminium complex $[Fe_2\{\mu-\eta^1:\eta^3-C(Tol)=CHC=N(Me)(4-C_6H_4CF_3)\}(\mu-CO)(CO)(Cp)_2][SO_3CF_3]$ (**4**) with NaBH_4 and NBu$_4^n$CN afford the allylidene $[Fe_2\{\mu-C(Tol)C(H)=C(H)N(Me)(C_6H_4CF_3)\}(\mu-CO)(CO)(Cp)_2]$ (**5**) and the cyanoallylidene $[Fe_2\{\mu-C(Tol)C(H)=C(CN)N(Me)(C_6H_4CF_3)\}(\mu-CO)(CO)(Cp)_2]$ (**6**), respectively. Analogously, the diruthenium vinyliminium complex $[Ru_2\{\mu-\eta^1:\eta^3-C(SiMe_3)=CHC=N(Me)(CH_2Ph)\}(\mu-CO)(CO)(Cp)_2][SO_3CF_3]$ (**7**) reacts with NBu$_4^n$CN to give $[Ru_2\{\mu-\eta^1:\eta^3-C(SiMe_3)CHC(CN)N(Me)(CH_2Ph)\}(\mu-CO)(CO)(Cp)_2]$ (**8**).

Finally, cyanide addition to $[Fe_2\{\mu-\eta^1:\eta^3-C(COOMe)=C(COOMe)C=N(Me)(Xyl)\}(\mu-CO)(CO)(Cp)_2][SO_3CF_3]$ (**2e**) (Xyl = 2,6-Me_2C_6H_3), yields the cyano-functionalized bis-alkylidene complex $[Fe_2\{\mu-\eta^1:\eta^2-C(COOMe)C(COOMe)(CN)CN(Me)(Xyl)\}(\mu-CO)(CO)(Cp)_2]$ (**10**). The molecular structures of **3a** and **9a** have been elucidated by X-ray diffraction.
© 2006 Elsevier B.V. All rights reserved.

Keywords: Vinyliminium; Diiron complexes; Allylidene; Vinylalkylidene; Cyanide addition

1. Introduction

Di- and polynuclear metal complexes are subject of interest since the presence of bridging ligands and cooperation among close metal centres is a potential source of unique reactivity [1]. Our interest in the area has concerned the chemistry of the diiron bridging vinyliminium complexes **1** and **2** (Chart 1). These latter have been obtained by insertion of mono and di-substituted alkynes, respectively, in the metal–carbyne bond of the parent μ-amino-carbyne complexes $[Fe_2\{\mu-C=N(Me)(R)\}(\mu-CO)(CO)(NCMe)(Cp)_2][SO_3CF_3]$ [2].

The bridging vinyliminium ligands display a remarkable electrophilic character and have been shown to react with NaBH_4 undergoing hydride addition [3]. The addition occurs selectively at the iminium carbon (C_α), except for the complexes (**1f–h**) in which bulky Xyl group (Xyl = 2,6-Me_2C_6H_3) was found to inhibit hydride attack at C_α and direct the addition to the less hindered C_β [3a]. Attempts to extend our studies to the reactions with carbon nucleophiles (*i.e.* lithium organyls) have evidenced a different reactivity consisting in the deprotonation of the C_β–H of the vinyliminium ligand. The deprotonated intermediates

* Corresponding author.
  E-mail address: valerio.zanotti@unibo.it (V. Zanotti).

R   R'
Me   SiMe$_3$ **1a**
Me   CH$_2$OH   **1b**
CH$_2$Ph   Tol   **1c**
CH$_2$Ph   COOMe   **1d**
CH$_2$Ph   SiMe$_3$ **1e**
Xyl   COOMe   **1f**
Xyl   Tol   **1g**
Xyl   SiMe$_3$ **1h**

R   R'
Me   Me   **2a**
Me   Ph   **2b**
CH$_2$Ph   Me   **2c**
CH$_2$Ph   COOMe   **2d**
Xyl   COOMe   **2e**
Xyl   Me   **2f**
Xyl   Et   **2g**
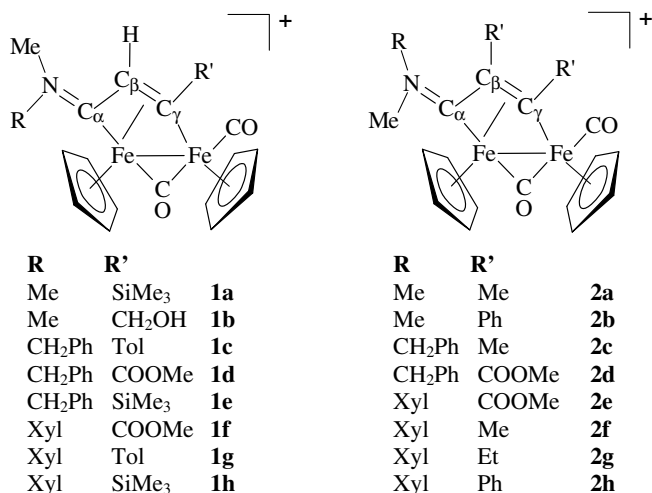Xyl   Ph   **2h**

Chart 1.

have been shown to rearrange affording new mono and polynuclear complexes [4]. On the other hand, type **2** complexes, which do not contain acidic C$_\beta$–H hydrogens, have been found to react with LiR undergoing nucleophilic addition at the C$_5$H$_5$ ligand, rather than at the bridging vinyliminium. Initial attack is followed by an intramolecular rearrangement, which involves hydride migration from the cyclopentadiene ring (C$_5$H$_5$R) to the vinyliminium ligand affording μ-vinylcarbene complexes [5].

Herein, we report on the reactions of **1–2**, including a similar diruthenium complex [6] with cyanide, in order to determine to which extent the reactivity of the bridging ligand is influenced by steric and electronic features of the substituents (R and R′). The cyanide is a 'stabilized carbanion' and, because of its lower basicity compared to other carbanions, is the ideal candidate to give nucleophilic addition at the bridging vinyliminium ligand, in spite of the acidic character of C$_\beta$–H.

A further reason to investigate the functionalization of the bridging ligand by cyanide is the high interest of the cyanocarbon transition metal chemistry, due to various potential applications in the field of new materials and organic synthesis [7].
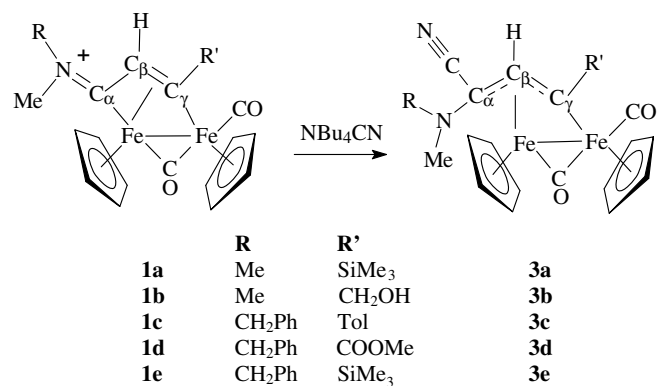
2. Results and discussion

2.1. Cyanide addition to vinyliminium complexes containing acidic C$_\beta$–H hydrogen

The vinyliminium complexes [Fe$_2$\{μ-η^1:η^3-C(R′)=CHC=N(Me)(R)\}(μ-CO)(CO)(Cp)$_2$][SO$_3$CF$_3$] (**1a–e**), containing the acidic C$_\beta$–H hydrogen, react with (NBu$_4^n$)(CN), in CH$_2$Cl$_2$ solution, affording the complexes **3a–e**, in about 80–90% yields (Scheme 1).

It is worth noting that cyanide exclusively attacks the iminium carbon, rather than following other reaction modes, including C$_\beta$–H proton removal, CO displacement or addition at other sites of the μ-ligand. The nature of

complexes **3a–e** has been determined by elemental analyses, spectroscopy and X-ray diffraction for **3a**. Two crystallographically independent but chemically equivalent molecules have been found in the crystal (see Section 4). The ORTEP molecular diagram of one of them is shown in Fig. 1. Relevant bond lengths and angles are reported in Table 1. It is worth noting that all the corresponding bond distances in the two molecules are equal within experimental errors. Minor differences are observable in the conformation of the ancillary groups. The molecular stereogeometry of **3a** is consistent with that of the parent cation **1a**, in which the C$_\alpha$–C$_\beta$–C$_\gamma$ unit of the vinyliminium ligand is bonded to the Fe$_2$ unit in the non-conventional mode shown in Scheme 1. The information conveyed by the X-ray structure is primarily that CN$^-$ attacks the more electrophilic C$_\alpha$ carbon [C(5)]. The generation of a C–C bond turns the vinyliminium ligand into an allylidene derivative, as one can infer from the double bond character and the substantial equivalence of the C$_\alpha$–C$_\beta$–C$_\gamma$ distances in both molecules [C(5)–C(4) 1.447 and 1.449(3) Å; C(4)–C(3) 1.414 and 1.419(3) Å]. Also the coordination interactions Fe–(C$_\alpha$–C$_\beta$–C$_\gamma$) exhibit minor differences [Fe(1)–C(5) 2.068 and 2.077(2) Å; Fe(1)–C(4) 2.012 and 2.007(2) Å; Fe(1)–C(3) 2.045 and 2.037(2) Å].

R   R'
1a   Me   SiMe$_3$ **3a**
1b   Me   CH$_2$OH   **3b**
1c   CH$_2$Ph   Tol   **3c**
1d   CH$_2$Ph   COOMe   **3d**
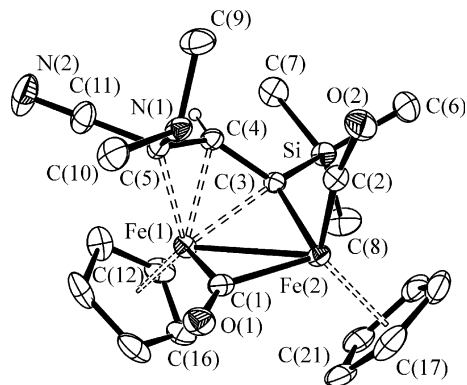**1e**   CH$_2$Ph   SiMe$_3$ **3e**

Scheme 1.

Fig. 1. ORTEP drawing (ellipsoids at 30% probability) of one of the two conformers of **3a**. Only the allylic C$_\beta$ hydrogen is shown.

Table 1
Selected bond lengths (Å) and angles (°) for **3a** and **9a**

	3a[a]	**9a**
Fe(1)–C(1)	1.910(2) [1.909(2)]	1.914(2)
Fe(1)–C(3)	2.045(2) [2.037(2)	2.027(1)
Fe(1)–C(4)	2.012(2) [2.007(2)]	2.037(1)
Fe(1)–C(5)	2.068(2) [2.077(3)]	2.059(1)
Fe(2)–C(1)	1.935(2) [1.932(3)]	1.927(1)
Fe(2)–C(2)	1.742(2) [1.753(3)]	1.765(2)
Fe(2)–C(3)	1.969(2) [1.973(2)]	1.975(2)
Fe(1)–Fe(2)	2.5408(5) [2.5488(5)]	2.5327(3)
C(1)–O(1)	1.168(3) [1.176(3)]	1.173(2)
C(2)–O(2)	1.154(3) [1.150(3)]	1.143(2)
C(5)–N(1)	1.445(3) [1.431(3)]	1.437(2)
C(9)–N(1)	1.470(3) [1.461(3)]	1.469(2)
C(10)–N(1)	1.459(3) [1.463(3)]	1.462(2)
C(3)–C(4)	1.414(3) [1.419(3)]	1.418(2)
C(4)–C(5)	1.447(3) [1.449(3)]	1.469(2)
C(5)–C(11)/C(5)-C(8)	1.465(4) [1.470(4)]	1.467(2)
C(11)–N(2)/C(8)-N(2)	1.137(3) [1.133(4)]	1.143(2)
C(3)–Si	1.883(2) [1.886(2)]	–
N(2)–C(11)/N(2)-C(8)	1.137(3) [1.133(4)]	1.143(2)
Fe(1)–C(Cp)(av)[b]	2.082 [2.106]	2.102
Fe(2)–C(Cp)(av)[b]	2.138 [2.130]	2.114
Fe(1)–C(1)–O(1)	141.3(2) [140.0(2)]	140.9(1)
Fe(2)–C(1)–O(1)	135.4(2) [136.2(2)]	136.1(1)
C(3)–C(4)–C(5)	125.5(2) [125.5(2)]	119.2(1)
N(1)–C(5)–C(4)	122.1(2) [122.5(2)]	120.0(1)
C(5)–C(8)–N(2)	–	175.2(2)
C(5)–C(11)–N(2)	177.2(3) [178.0(4)]	–

[a] Values in parentheses refer to the second conformer in the asymmetric unit.
[b] Main image of the Cp ligand.

The spectroscopic data of **3a–e** are in good agreement with the solid state structure. Their infrared spectra, in CH_2Cl_2 solution, exhibit absorptions for the terminal and bridging carbonyls (*e.g.* at 1969 and 1787 cm^{-1} for **3a**) and a $\nu(CN)$ absorption at about 2190 cm^{-1}. The NMR spectra of **3a–b**, in CDCl$_3$ solution, show the presence of a single isomer. Since the CN$^-$ addition at C_α could occur either on the same side of C_β–H or in the opposite one, generating *syn* and *anti* isomers, respectively, we conclude that the reaction is stereoselective and assume that the geometry adopted in solution is that observed in the solid state with the CN group *syn* to the C_β–H. The ^{1}H NMR spectra of **3a–b** show two distinct resonances for the NMe$_2$ protons (*e.g.* at δ 2.31 and 1.71 ppm for **3a**). Their inequivalence suggests that free rotation around the C_α–N bond is inhibited for steric reasons, because the C_α–N interaction does not display double bond character [C(5)–N(1) 1.445 and 1.431(3) Å]. In fact, the geometry observed for **3a** evidences that the CH$_3$ groups in NMe$_2$ would bump into the terminal CO ligand [C(2)–O(2)] upon rotation around the C(5)–N(1) axis [N(1)···C(2) contact 2.761(3) and 2.695(4) Å].

Other NMR features include the typical resonances for C_α, C_β and C_γ of the allylidene skeleton (*e.g.* for **3a** at 67.6 ppm, 86.5 ppm, 194.5 ppm, respectively) and the resonance of the cyanide carbon, at about 121 ppm.

Complexes **3c–e** exist as a mixture of two isomers in about 1:5 ratio. These are due to the lack of free orienta-

tion of the methyl and benzyl groups around the C_α–N bond, as just discussed for the NMR non-equivalence of the NMe$_2$ methyl groups in **3a–b**. NOE experiments on the major isomer of **3e** suggest that the most favourable geometry is that with the methyl and benzyl groups pointing toward the bridging and terminal CO, respectively (Chart 2). Indeed, irradiation of the NMe resonance of the major isomer (1.63 ppm) resulted in significant enhancement of one Cp resonance (5.03 ppm), whereas irradiation of the NMe resonance of the secondary isomer (2.43 ppm) gave no effect on the Cp resonances. Moreover, regarding the minor isomer, NOE effect was detected on the CH$_2$ benzyl protons by irradiating the Cp resonance at 4.97 ppm.

The reactions described in Scheme 1 parallel the corresponding addition of NaBH$_4$ [3a]. Indeed, complexes **1a–e** undergo hydride attack at the C_α affording the corresponding μ-allylidene complexes [Fe$_2$\{μ-η^1:η^3–C(R′)CH-C(H)N(Me)(R)\}(μ-CO)(CO)(Cp)$_2$] (R = Me, CH$_2$Ph), similar to **3a–e**. In both cases nucleophilic attack occurs exclusively at the iminium carbon and is stereospecific. However, the orientation of the entering groups is different: hydride is found *anti* with respect to the C_β–H, whereas cyanide is *syn*. The conformational freedom of the NMe(R) substituent is consequently different in the two cases, with hindered rotation observed only in the complexes obtained by CN$^-$ addition.

It is worth noting that the reaction described above points out the similarities between H$^-$ (from NaBH$_4$) and CN$^-$ (from NBu$_4$CN) as far as nucleophilic additions at bridging ligands in cationic diiron complexes [8] are concerned.

By contrast with the reactions shown in Scheme 1, the complexes [Fe$_2$\{μ-η^1:η^3-C(R′)=CHC=N(Me)(Xyl)\}(μ-CO)(CO)(Cp)$_2$][SO$_3$CF$_3$] (R′ = CO$_2$Me (**1f**); R′ = Tol (**1g**); R′ = SiMe$_3$ (**1h**)), characterized by the presence of the bulkier Xyl (2,6-Me$_2$C$_6$H$_3$) group, react with cyanide yielding alkynyl complexes or fragmentation of the dinuclear precursor (Scheme 2). The reaction products are those previously observed by deprotonation of **1f–h** by NaH [4]. Therefore, the presence of the Xyl group in **1f–h** inhibits the attack at the iminium carbon and favours the C_β–H proton removal.

The result is unexpected and markedly different from what observed in the corresponding reactions with NaBH$_4$:
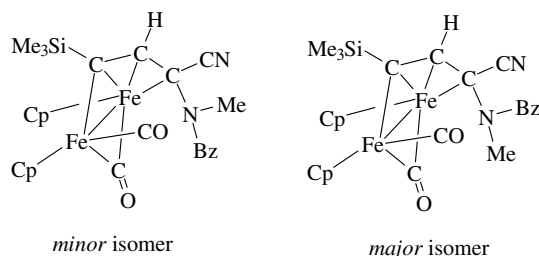

minor isomer   *major* isomer

Chart 2. isomers due to orientations of the N-substituents for **3e**.

1f–h were found to undergo hydride addition at C_β affording bis–alkylidene complexes of the type $[Fe_2\{\mu-\eta^1:\eta^2-C(R')CH_2CN(Me)(Xyl)\}(\mu-CO)(CO)(Cp)_2]$. The reason why CN^- reacts removing the C_β–H hydrogen rather than giving addition at the C_β carbon remains unclear. The steric influence exerted by the Xyl group is quite evident, but electronic effects due to its electron-withdrawing character should also be taken into account. For a better discrimination between electronic and steric effects, the reactivity of $[Fe_2\{\mu-\eta^1:\eta^3-C(Tol)=C(H)C=N(Me)(4-C_6H_4–CF_3)\}(\mu-CO)(CO)(Cp)_2][SO_3CF_3]$ (**4**), in which a *para*-trifluoro methyl benzene ($R = 4-C_6H_4–CF_3$) replaces the Xyl group, has been investigated. The synthesis of **4**, which is a novel compound, is detailed in Section 4. The *p*-$C_6H_4–CF_3$ group is less sterically demanding than Xyl, but a better electron-withdrawer. The reactions of **4** with $NaBH_4$ and NBu_4^tCN have shown that, in both cases, the nucleophilic attack occurs selectively at C_α (Scheme 3), suggesting that the steric bulk of the N substituents is dominant. Compounds $[Fe_2\{\mu-C(Tol)C(H)=C(H)N(Me)(C_6H_4CF_3)\}(\mu-CO)(CO)-(Cp)_2]$ (**5**) and $[Fe_2\{\mu-C(Tol)C(H)=C(CN)N(Me)(C_6H_4-CF_3)\}(\mu-CO)(CO)(Cp)_2]$ (**6**) have been characterized by IR and ^1H, ^{13}C and ^{19}F NMR spectroscopy. Complex **5** is analogous to previously reported compounds [3a], whereas complex **6** resembles **3a–e**.

We have recently shown that diruthenium vinyliminium complexes analogous to the diiron species **1** and **2** can also be obtained [6]. Their chemistry parallels that of their diiron counterparts, however some minor differences, regarding the geometry of the complexes and the reactivity of the terminally coordinated ligands have been evidenced. Thus, in order to evidence possible effects due to the presence of ruthenium in the place of iron, the reaction of the diruthenium complex **7** with NBu_4^nCN has been investigated. The result is the quantitative formation of the cyano-functionalized allylidene complex **8**, analogous to **3e** (Scheme 4).

Therefore, ruthenium does not produce any noticeable difference in the reactivity of the bridging ligand. The spectroscopic data of **8** are similar to those of the diiron counterpart **3e**, although only one isomer was observed. Moreover, the reaction has also been performed with ^{13}C-enriched cyanide (by using a 10:1 mixture of NBu_4CN and $K^{13}CN$, 99% ^{13}C, from Aldrich). The corresponding reaction product **8** has evidenced, in the ^{13}C NMR spec-
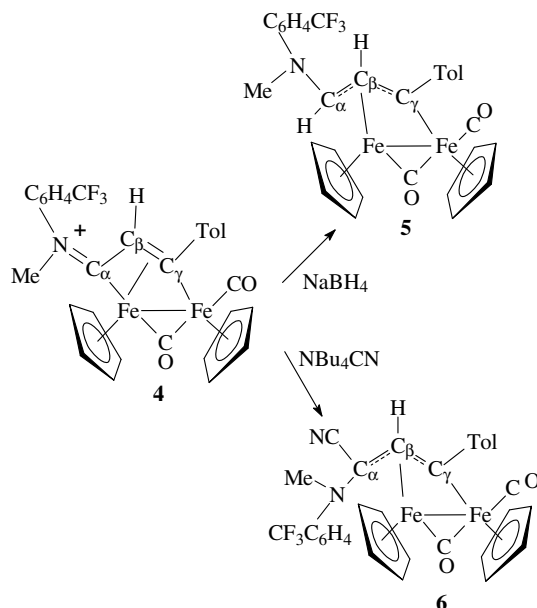
Scheme 3.
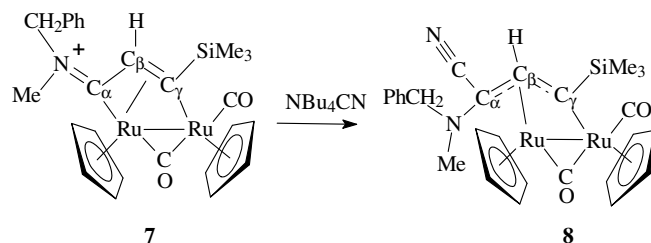
Scheme 4.

trum, an intense resonance at 121.9 ppm (C_α–CN), and a doublet at δ 67.9 ppm ($^1J_{CC} = 63.3$ Hz, C_α), indicating that addition occurs selectively at the iminium carbon (C_α).

2.2. Cyanide addition to disubstituted vinyliminium complexes in the absence of C_β–H

Compounds **2a–d** rapidly react with a slight excess of NBu_4^nCN, in CH_2Cl_2 solution, affording the bridging cyano-functionalized allylidene complexes $[Fe_2\{\mu-\eta^1:\eta^3-C(R')C(R')C(CN)N(Me)(R)\}(\mu-CO)(CO)(Cp)_2]$ (**9a–d**), in about 80–90% yields (Scheme 5).

Scheme 2.

Scheme 5.

	R	R'	
2a	Me	Me	9a
2b	Me	Ph	9b
2c	CH₂Ph	Me	9c
2d	CH₂Ph	COOMe	9d
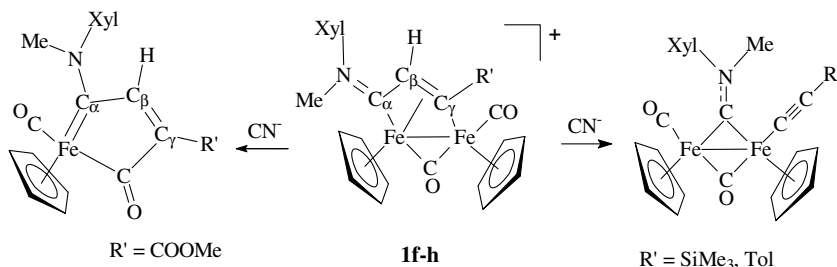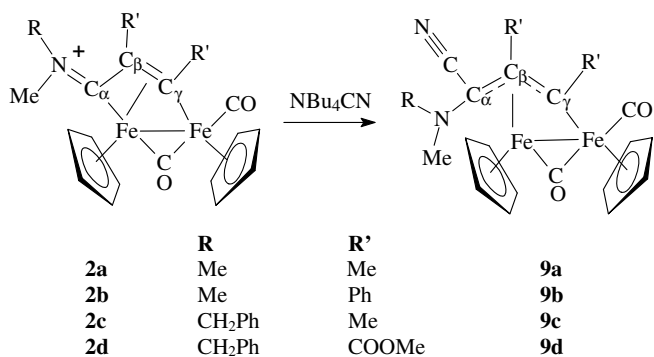
The structure of **9a** has been determined by X-ray diffraction: the ORTEP molecular diagram is shown in Fig. 2 and relevant bond lengths and angles are reported in Table 1. The molecular geometry is similar to that of **3a** discussed above. The presence of a methyl substituent at C_β [C(4)–C(7)] has not influenced the configuration around C_α [C(5)] and the CN group is oriented *syn* with respect to C_β-Me. The bond parameters of interest are strictly equivalent to the corresponding ones in **3a**. It is worth noting that also the NMe_2 group is oriented as in **3a**.

The spectroscopic data for **9a–b** are very similar to those of **3a–e**. Again, for **9a–b** the NMR data indicate the presence of a single isomer and the non-equivalence of the two N-bonded methyl groups, whereas two isomers are observed in solution, for the complexes **9c–d**.

The addition of cyanide at the iminium carbon of **2a–d** is in accord with the observation that, in the absence of steric protection offered by the Xyl group, nucleophilic attack occurs selectively at the iminium carbon (C_α). Conversely, the complexes [Fe₂{μ-η¹:η³-C(R')=C(R')C=N(Me)(Xyl)}-(μ-CO)(CO)(Cp)₂][SO₃CF₃] (R' = Me (**2f**); R' = Et (**2g**); R' = Ph (**2h**)), containing the Xyl substituent, do not react with CN⁻. In this case, the iminium carbon is not accessible, neither deprotonation can occur, because of the
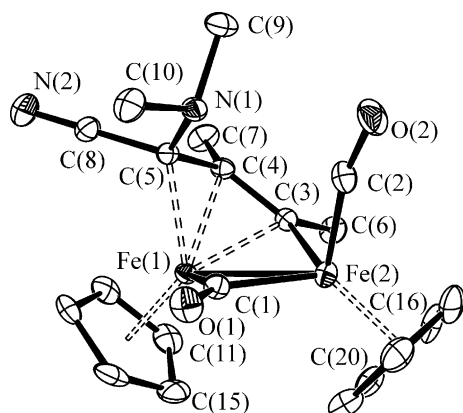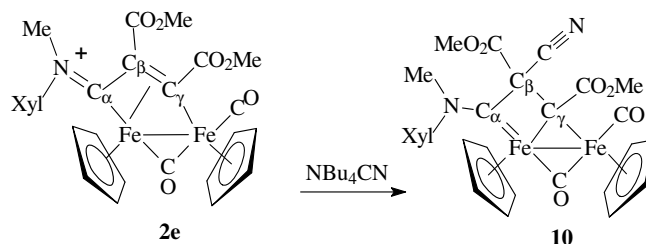
absence of acidic C_β–H. An exception among these unreactive vinyliminium complexes is represented by [Fe₂{μ-η¹:η³-C(COOMe)=C(COOMe)C=N(Me)(Xyl)}(μ-CO)-(CO)(Cp)₂][SO₃CF₃] (**2e**). Indeed, the latter compound reacts with NBu₄ⁿCN, in CH₂Cl₂ solution, yielding the cyano-functionalized bis-alkylidene complex **10** (Scheme 6). Compound **10**, fully characterized by spectroscopy and elemental analysis, is the result of selective cyanide addition at the C_β position and consequent adjustment of the coordination mode of the bridging ligand, which remains connected to the Fe atoms through the C_α and C_γ carbons. Both carbons exhibit carbene character: the former is an amino carbene ligand, terminally coordinated, whereas the latter is a bridging alkylidene. This bis-alkylidene coordination mode appears very stable and has been previously found upon hydride addition at C_β [3] or rearrangements promoted by C_β–H proton removal [4] in μ-vinyliminium complexes.

An explanation of the higher reactivity of **2e**, compared to **2f–h**, should be related to the electron-withdrawing substituents (COOMe) at both C_β and C_γ.

The infrared spectrum of **10** (in CH₂Cl₂ solution) exhibits the usual pattern consisting of two strong absorptions for terminal and bridging carbonyls (1947, 1777 cm⁻¹), and, in addition, absorptions attributable to C≡N (at 2175 cm⁻¹) and to the carboxylate (at 1733 and 1683 cm⁻¹). The NMR spectra show only one isomer, indicating that the addition is stereo- and regio-selective; the ¹³C NMR spectrum exhibits the resonances relative to C_α, C_β and C_γ in the typical regions for an aminocarbene (δ 252.7 ppm), a quaternary sp³ carbon (81.5 ppm) and a bridging alkylidene bound to a carboxylate (129.4 ppm), respectively.

Labelling experiments with ¹³C-enriched CN⁻ confirms that cyanide addition occurs selectively at C_β: the ¹³C NMR spectrum of the ¹³C labelled product **10** displays doublets at δ 129.4 ppm ($^2J_{CC}$ = 5.0 Hz, C_γ) and 81.5 ppm ($^1J_{CC}$ = 67.2 Hz, C_β), and an intense singlet at 116.5 ppm (C_β–CN).

Since the C_α N(Me)(Xyl) moiety in **10** shows aminocarbene character, free rotation around the C_α–N bond is not allowed, due to its partial double bond character. Two isomers could consequently arise, according to the orientations of the Me and Xyl substituents. Since only one isomer is observed, we assume that this is the one with the N*Me* group pointing toward the C_β substituent. This conformation is suggested by NOE experiments, which

Fig. 2. ORTEP drawing (ellipsoids at 30% probability) of **9a**. Hydrogen atoms have been omitted for clarity.

Scheme 6.

evidence enhancement only of one methyl group of the Xyl substituent (at 2.12 ppm) upon irradiation of the Cp resonance at 4.19 ppm. A similar geometry has been previously observed in the X-ray structure of the related bis-alkylidene complex [Fe$_2$\{μ-η^1:η^2-C(Et)C(Et)(H)CN-(Me)(Xyl)\}(μ-CO)(CO)(Cp)$_2$] [3b].

Although no structural investigation has been carried out on complex **10**, it is likely that the addition of CN$^-$, which generates a stereogenic centre at C$_\beta$, is completely stereoselective and occurs in the side opposite to the Cp ligands, as previously observed for the addition of hydride to similar complexes [3].

3. Conclusions

Diiron vinyliminium complexes undergo regio- and stereo-specific additions by cyanide ion, under mild conditions. The addition occurs normally at the iminium carbon (C$_\alpha$), affording novel bridging cyano-functionalized allylidene complexes, and is not influenced by the nature of the substituent at C$_\beta$, neither by the presence of ruthenium in place of iron. Conversely, in the presence of the xylyl substituent at the iminium nitrogen, the CN$^-$ addition to C$_\alpha$ is inhibited by steric reasons. Different outcomes are consequently observed: in the presence of C$_\beta$–H hydrogen, the cyanide ion promotes deprotonation; otherwise, the vinyliminium is simply unreactive, unless activated by the presence of electron-withdrawing substituents. In the latter case, CN$^-$ addition takes place selectively at C$_\beta$, affording a cyano-functionalized bis-alkylidene complex.

4. Experimental details

4.1. General

All reactions were carried out routinely under nitrogen, using standard Schlenk techniques. Solvents were distilled immediately before use under nitrogen from appropriate drying agents. Chromatography separations were carried out on columns of deactivated alumina (4% w/w water). Glassware was oven-dried before use. Infrared spectra were recorded on a Perkin–Elmer Spectrum 2000 FT-IR spectrophotometer and elemental analyses were performed on a ThermoQuest Flash 1112 Series EA Instrument. All NMR measurements were performed on Varian Gemini 300 and Mercury Plus 400 instruments. The chemical shifts for ^{1}H and ^{13}C were referenced to internal TMS. The spectra were fully assigned *via* DEPT experiments and ^{1}H,^{13}C correlation through gs-HSQC and gs-HMBC experiments [9]. All NMR spectra were recorded at 298 K; NMR signals due to a second isomeric form (where it has been possible to detect and/or resolve them) are italicized. NOE measurements were recorded using the DPFGSE-NOE sequence [10]. All the reagents were commercial products (Aldrich Co.) of the highest purity available and used as received, except for complexes **1a–h**, **2a–e**, and **7**, which were prepared by the published methods [2,6].

4.2. Synthesis of [Fe$_2$\{μ-η^1:η^3-C$_\gamma$(R')C$_\beta$(H)C$_\alpha$(CN)N(Me)(R)\}(μ-CO)(CO)(Cp)$_2$] (R = Me, R' = SiMe$_3$ (3a); R = Me, R' = CH$_2$OH (3b); R = CH$_2$Ph, R' = Tol (3c); R = CH$_2$Ph, R' = COOMe (3d); R = CH$_2$Ph, R' = SiMe$_3$ (3e))

A solution of **1a** (95 mg, 0.158 mmol), in CH$_2$Cl$_2$ (10 mL), was treated with NBu$^n_4$CN (64 mg, 0.239 mmol). After stirring at room temperature for 20 min, the mixture was filtered on alumina. Solvent removal, under reduced pressure, afforded **3a** as a brown microcrystalline powder. Yield: 64 mg (91%). Crystals suitable for X-ray analysis were collected by layering a CH$_2$Cl$_2$ solution of **3a** with petroleum ether, at −20 °C. Anal. Calc. for C$_{21}$H$_{26}$Fe$_2$N$_2$O$_2$Si: C, 52.74; H, 5.48; N, 5.86. Found: C, 52.80; H, 5.44; N, 5.98%. IR (CH$_2$Cl$_2$) v(C≡N) 2188 (m), v(CO) 1969 (vs), 1787 (s) cm^{-1}. ^{1}H NMR (CDCl$_3$) 4.94, 4.49 (s, 10H, Cp); 4.74 (s, 1H, C$_\beta$H); 2.32, 1.71 (s, 6H, NMe); 0.63 (s, 9H, SiMe$_3$). ^{13}C\{^{1}H\} NMR (CDCl$_3$) δ 264.9 (μ-CO); 212.2 (CO); 194.5 (C$_\gamma$); 121.1 (CN); 87.4, 84.6 (Cp); 86.5 (C$_\beta$); 67.6 (C$_\alpha$); 49.8, 42.2 (NMe); 3.6 (SiMe$_3$).

Compounds **3b–e** were obtained by the same procedure described for **3a**, by reacting NBu$^t_4$CN with **1b–e**, respectively.

3b: Yield (81%). Anal. Calc. for C$_{19}$H$_{20}$Fe$_2$N$_2$O$_3$: C, 52.33; H, 4.62; N, 6.42. Found: C, 52.27; H, 4.71; N, 6.33%. IR (CH$_2$Cl$_2$) v(C≡N) 2190 (m), v(CO) 1967 (vs), 1790 (s) cm^{-1}. ^{1}H NMR (CDCl$_3$) 5.94 (m, 2H, CH_2OH); 5.05 (s, 1H, C$_\beta$H); 4.89, 4.49 (s, 10H, Cp); 2.29, 1.73 (s, 6H, NMe). ^{13}C\{^{1}H\} NMR (CDCl$_3$) δ 264.2 (μ-CO); 212.8 (CO); 200.3 (C$_\gamma$); 121.0 (CN); 87.4, 85.6 (Cp); 49.3, 44.1 (NMe).

3c: Yield (78%). Anal. Calcd. for C$_{31}$H$_{28}$Fe$_2$N$_2$O$_2$: C, 65.06; H, 4.93; N, 4.90. Found: C, 65.05; H, 4.97; N, 4.81%. IR (CH$_2$Cl$_2$)v(C≡N) 2189 (m), v(CO) 1972 (vs), 1784 (s) cm^{-1}. ^{1}H NMR (CDCl$_3$) 7.55–7.18 (m, 9H, C$_6$H$_4$Me and Ph); 4.73, 4.71, *4.65, 4.62* (s, 10H, Cp); 4.71, 3.29 (d, 2H, $^2J_{HH}$ = 13 Hz, CH_2Ph); 4.47 (s, 1H, C$_\beta$H); 2.47, *2.43* (s, 3H, C$_6$H$_4$Me); 2.20, 1.70 (s, 3H, NMe); isomer ratio 7:1. ^{13}C\{^{1}H\} NMR (CDCl$_3$) δ 264.6 (μ-CO); *213.3*, 212.0 (CO); 200.9 (C$_\gamma$); 156.1 (ipso-C$_6$H$_4$Me); 135.4–126.8 (C$_6$H$_4$Me and Ph); 121.1, *121.0* (CN); 89.4, *86.3*, 86.1 (Cp); 81.6 (C$_\beta$); 65.7 (C$_\alpha$); *64.8*, 59.8 (CH$_2$Ph); 46.4, *39.8* (NMe); 21.1 (C$_6$H$_4$Me).

3d: Yield (82%). Anal. Calc. for C$_{26}$H$_{24}$Fe$_2$N$_2$O$_4$: C, 57.81; H, 4.48; N, 5.19. Found: C, 57.93; H, 4.50; N, 5.23%. IR (CH$_2$Cl$_2$) v(C≡N) 2191 (w), v(CO) 1982 (vs), 1795 (s), 1704 (m) cm^{-1}. ^{1}H NMR (CDCl$_3$) 7.29–7.09 (m, 5H, Ph); 4.90, *4.84*, 4.71, *4.61* (s, 10H, Cp); 4.86 (s, 1H, C$_\beta$H); 4.51, 3.24, *3.07, 2.95* (d, 2H, $^2J_{HH}$ = 12 Hz, CH_2Ph); 4.09, *4.05* (s, 3H, CO$_2$Me); *2.31*, 1.60 (s, 3H, NMe); isomer ratio 5:1. ^{13}C\{^{1}H\} NMR (CDCl$_3$) δ 262.4, 260.7 (μ-CO); 211.2, *210.9* (CO); 180.8, 180.7 (C$_\gamma$ and CO$_2$Me); 137.2, 129.9, 127.8, 126.9 (Ph); 120.8 (CN); 88.3, *88.3*, *87.1*, 86.8 (Cp); 80.6 (C$_\beta$); 64.7 (C$_\alpha$); 59.7 (CH$_2$Ph); 52.4, *52.2* (CO$_2$Me); 46.1, *38.6* (NMe).

3e: Yield (93%). Anal. Calc. for $C_{27}H_{30}Fe_2N_2O_2Si$: C, 58.50; H, 5.46; N, 5.05. Found: C, 58.60; H, 5.55; N, 4.87%. IR (CH_2Cl_2) $v(C\equiv N)$ 2188 (m), $v(CO)$ 1972 (vs), 1785 (s) cm^{-1}. ^1H NMR ($CDCl_3$) 7.32–7.08 (m, 5H, Ph); 5.03, *4.97*, 4.57, *4.50* (s, 10H, Cp); 4.78 (s, 1H, $C_\beta H$); 4.66, 3.26 (d, 2H, $^2J_{HH}$ = 13 Hz, CH_2Ph); *2.43*, 1.63 (s, 3H, NMe); 0.68, *0.58* (s, 9H, SiMe$_3$); isomer ratio 5:1. $^{13}C\{^1H\}$ NMR ($CDCl_3$) δ 264.6 (μ-CO); *213.1*, 211.9 (CO); 195.4, *194.3* (C_γ); 138.0, 130.6, 129.3, 127.8, 126.6 (Ph); 121.5 (CN); *87.6*, 87.5, *86.2*, 84.8 (Cp); 85.0 (C_β); 68.1 (C_α); *64.9*, 59.9 (CH$_2$Ph); 46.5, *40.1* (NMe); *3.6*, 3.5 (SiMe$_3$).

4.3. Synthesis of [Fe₂{μ-CN(Me)(p-C₆H₄CF₃)} (μ-CO)(CO)₂(Cp)₂][SO₃CF₃]

CN(p-C$_6$H$_4$CF$_3$) (1.00 g, 5.85 mmol) was added to a solution of [Fe$_2$(Cp)$_2$(CO)$_4$] (3.11 g, 8.79 mmol) in MeCN (100 mL), and the mixture was heated at reflux temperature for 24 h. Then, the solvent was removed under reduced pressure and the residue was dissolved in CH$_2$Cl$_2$ (50 mL). Hence, CH$_3$SO$_3$CF$_3$ (0.7 mL, 6.2 mmol) was added, and the mixture was stirred for 5 h. The resulting solution reduced in volume and treated with and diethyl ether (200 mL). A dark red precipitate, corresponding to [Fe$_2${μ-CN(Me)(p-C$_6$H$_4$CF$_3$)}(μ-CO)(CO)$_2$(Cp)$_2$][SO$_3$CF$_3$], was isolated. Yield: 1.74 g (45%). Anal. Calc. for C$_{23}$H$_{17}$F$_6$Fe$_2$NO$_6$S: C, 41.78; H, 2.59; N, 2.12. Found: C, 41.69; H, 2.44; N, 2.16%. IR (CH$_2$Cl$_2$) $v(CO)$ 2024 (vs), 1994 (s), 1840 (s), $v(\mu$-CN) 1539 (m). ^1H NMR (CDCl$_3$) δ 8.02–7.67 (m, 4H, C$_6$H$_4$); 5.45, 4.74 (s, 10H, Cp); 4.55 (s, 3H, NMe). $^{13}C\{^1H\}$ NMR (CDCl$_3$) δ 326.4 (μ-C); 252.8 (μ-CO); 208.5, 207.2 (CO); 152.5 (ipso-C$_6$H$_4$); 127.7, 126.1 (C$_6$H$_4$); 90.4, 90.0 (Cp); 57.2 (NMe). $^{19}F\{^1H\}$ NMR (CDCl$_3$) δ −63.0 (s, 3 F, p-C$_6$H$_4$CF$_3$); −78.5 (s, 3 F, CF$_3$SO$_3$).

4.4. Synthesis of [Fe₂{μ-CN(Me)(p-C₆H₄CF₃)} (μ-CO)(CO)(NCMe)(Cp)₂][SO₃CF₃]

A solution of [Fe$_2${μ-CN(Me)(p-C$_6$H$_4$CF$_3$)}(μ-CO)(CO)$_2$(Cp)$_2$][SO$_3$CF$_3$] (300 mg, 0.453 mmol), in MeCN (20 mL), was treated with Me$_3$NO (44 mg, 0.587 mmol), and the resulting mixture was stirred for 30 min. Then, the solvent was removed under reduced pressure, the residue was dissolved in CH$_2$Cl$_2$ (10 mL) and filtered through a celite pad. Removal of the solvent gave a brown powder. Yield: 275 mg (90%). Anal. Calc. for C$_{24}$H$_{20}$F$_6$Fe$_2$N$_2$O$_5$S: C, 42.76; H, 2.99; N, 4.16. Found: C, 42.81; H, 3.04; N, 4.05%. IR (CH$_2$Cl$_2$)$v(CO)$ 1985 (vs), 1819 (s), $v(\mu$-CN) 1524 (m). ^1H NMR (CDCl$_3$) 7.93–7.66 (m, 4H, C$_6$H$_4$); *5.07*, 4.75, 4.39, *4.22* (s, 10H, Cp); 4.87, *4.57* (s, 3H, NMe); 1.98 (s, 3H, NCMe). α/β ratio 3:2. $^{13}C\{^1H\}$ NMR (CDCl$_3$) δ 337.9, 337.6 (μ-C); *264.6*, 264.4 (μ-CO); 211.5, *210.5* (CO); 153.0, *152.5* (ipso-C$_6$H$_4$); 130.5, 130.1 (NCMe); 127.5, 127.3, 126.4 (C$_6$H$_4$); 88.8, 88.3, 87.3, 86.7 (Cp); *56.3*, 55.6 (NMe); 4.00 (NCMe). $^{19}F\{^1H\}$ NMR (CDCl$_3$) −62.7, −62.8 (s, 3 F, p-C$_6$H$_4$CF$_3$); −78.5 (s, 3 F, CF$_3$SO$_3$).

4.5. Synthesis of [Fe₂{μ-η¹:η³-Cγ(Tol)=Cβ HCα = N(Me)(p-C₆H₄CF₃)}(μ-CO)(CO)(Cp)₂] [SO₃CF₃] (4)

Compound [Fe$_2${μ-CN(Me)(p-C$_6$H$_4$CF$_3$)}(μ-CO)(CO)(NCMe)(Cp)$_2$][SO$_3$CF$_3$] (200 mg, 0.297 mmol) was dissolved in CH$_2$Cl$_2$ (25 mL), treated with HC$\equiv$CTol (0.33 mmol) and heated at boiling temperature for 4 h. Solvent removal and chromatography of the residue on an alumina column, with MeOH as eluent, gave a brown band corresponding to **4**. Yield: 156 mg (70%). Anal. Calc. for C$_{31}$H$_{25}$F$_6$Fe$_2$NO$_5$S: C, 49.69; H, 3.36; N, 1.87. Found: C, 49.78; H, 3.45; N, 1.79%. IR (CH$_2$Cl$_2$) $v(CO)$ 1992 (vs), 1813 (s), $v(C_\alpha N)$ 1607 (m). ^1H NMR (CDCl$_3$) 7.84–7.26 (m, 8H, C$_6$H$_4$CF$_3$ and C$_6$H$_4$Me); 5.26, *5.02*, 4.94, *4.85* (s, 10H, Cp); 4.38 (s, 1H, C$_\beta$H); *4.30*, 3.69 (s, 3H, NMe); 2.37 (s, 3H, C$_6$H$_4$*Me*). Z/E ratio 4:3. $^{13}C\{^1H\}$ NMR (CDCl$_3$) δ 255.5, 254.2 (μ-CO); 231.6, 229.9 (C_α); 209.5, *209.4* (CO); 207.5, *205.8* (C_γ); 153.3, 153.0 (ipso-C$_6$H$_4$Me); 148.1–122.5 (*C$_6$H$_4$CF$_3$ + C$_6$H$_4$Me*); 91.9, *91.5*, *89.0*, 88.5 (Cp); 56.1, 55.8 (C$_\beta$); 55.0, 52.3 (NMe); 20.9 (C$_6$H$_4$*Me*).

4.6. Synthesis of [Fe₂{μ-η¹:η³-Cγ(Tol)Cβ(H)=Cα (H)N(Me)(p-C₆H₄CF₃)}(μ-CO)(CO)(Cp)₂] (5)

Complex **4** (100 mg, 0.134 mmol) was dissolved in THF (10 mL) and treated with NaBH$_4$ (27 mg, 0.711 mmol). The mixture was stirred for 15 min. Then, the solvent was removed, the residue was dissolved in CH$_2$Cl$_2$ (10 mL), and filtered on alumina. Complex **5** was obtained as orange powder upon removal of the solvent. Yield: 64 mg (80%). Anal. Calc. for C$_{30}$H$_{26}$F$_3$Fe$_2$NO$_2$: C, 59.93; H, 4.36; N, 2.33. Found: C, 60.03; H, 4.41; N, 2.27%. IR (CH$_2$Cl$_2$) $v(CO)$ 1958 (vs), 1777 (s). ^1H NMR (CDCl$_3$) 7.76–7.32 (m, 8H, C$_6$H$_4$CF$_3$ and C$_6$H$_4$Me); 4.67 (d, 1H, $^3J_{HH}$ = 8.42 Hz, C$_\beta$H); 4.51, 4.49 (s, 10H, Cp); 2.80 (s, 3H, NMe); 2.49 (s, 3H, C$_6$H$_4$*Me*); 1.54 (d, 1H, $^3J_{HH}$ = 8.42 Hz, C$_\alpha$H). $^{13}C\{^1H\}$ NMR (CDCl$_3$) δ 263.0 (μ-CO); 214.9 (CO); 202.1 (C_γ); 157.7 (ipso-C$_6$H$_4$Me); 153.0 (ipso-C$_6$H$_4$CF$_3$); 134.6-124.2 (C$_6$H$_4$Me); 88.9, 85.0 (Cp); 84.5 (C$_\alpha$); 74.5 (C$_\beta$); 49.5 (NMe); 21.1 (C$_6$H$_4$*Me*). $^{19}F\{^1H\}$ NMR (CDCl$_3$) −141.4 (s, 3 F, p-C$_6$H$_4$CF$_3$).

4.7. Synthesis of [Fe₂{μ-η¹:η³-Cγ(Tol)Cβ(H)Cα(CN)N-(Me)(p-C₆H₄CF₃)}(μ-CO)(CO)(Cp)₂] (6)

A solution of **4** (90 mg, 0.120 mmol), in CH$_2$Cl$_2$ (10 mL), was treated with NBu$_4^n$CN (42 mg, 0.157 mmol), and the resulting mixture was stirred for 20 min. Then, the solution was filtered through an alumina pad. Complex **6** was obtained as an orange powder upon removal of the solvent. Yield: 275 mg (90%). Anal. Calc. for C$_{31}$H$_{25}$F$_3$Fe$_2$N$_2$O$_2$: C, 59.46; H, 4.02; N, 4.47. Found: C, 59.56; H, 4.08; N, 4.39%. IR (CH$_2$Cl$_2$)$v(C\equiv N)$ 2195 (w), $v(CO)$ 1972 (vs), 1788 (s). ^1H NMR (CDCl$_3$) 7.79–6.93 (m, 8H, C$_6$H$_4$CF$_3$ and C$_6$H$_4$Me); 4.80, 4.79, 4.62, 4.61 (s, 10H, Cp); 3.38 (s, 1H, C$_\beta$H); 3.19, 2.60 (s, 3H, NMe);

2.49, 2.48 (s, 3H, C_6H_4Me). Isomer ratio 1:1. $^{13}C\{^1H\}$ NMR (CDCl₃) δ 260.1 (μ-CO); 212.8, 211.0 (CO); 202.1, 200.3 (C_γ); 156.2 (ipso-C_6H_4Me); 153.6 (ipso-$C_6H_4CF_3$); 149.9–124.3 (C_6H_4Me and Ph); 123.0, 122.8 (CN); 117.9, 115.8 (C_β); 90.0, 86.5, 86.4 (Cp); 86.6, 85.8 (C_α); 48.1, 42.5 (NMe); 21.1 (C_6H_4Me). $^{19}F\{^1H\}$ NMR (CDCl₃) −61.6, −61.8 (s, 3 F, p-$C_6H_4CF_3$).

4.8. Synthesis of $[Ru_2\{\mu\text{-}\eta^1\text{:}\eta^3\text{-}C_\gamma$-$(SiMe_3)C_\beta(H)C_\alpha(CN)N(Me)(CH_2Ph)\}$ $(\mu\text{-}CO)(CO)(Cp)_2]$ (8)

NBu$_4^n$CN (40.0 mg, 0.149 mmol) was added to a solution of **7** (64 mg, 0.083 mmol), in CH₂Cl₂ (15 mL), and the solution stirred for 20 min. Solvent removal and chromatography on an alumina column, with CH₂Cl₂ as eluent, gave **8** as an orange fraction. Yield: 47 mg (88%). Anal. Calc. for $C_{27}H_{30}N_2O_2Ru_2Si$: C, 50.30; H, 4.69; N, 4.34. Found: C, 50.59; H, 4.87; N, 4.21%. IR (CH₂Cl₂) ν(C≡N) 2189 (m), ν(CO) 1971 (vs), 1786 (s) cm^{-1}. ^1H NMR (CDCl₃) δ 7.01–7.30 (m, 5H, Ph); 5.34, 4.90 (s, 10H, Cp); 4.83 (s, 1H, C_βH); 4.39, 3.21 (d, 2H, $^2J_{HH}$ = 12.6 Hz, CH_2Ph); 1.88 (s, 3H, NMe); 0.30 (s, 9H, SiMe₃). $^{13}C\{^1H\}$ NMR (CDCl₃) δ 237.3 (μ-CO); 200.5 (CO); 176.6 (C_γ); 137.9 (ipso-Ph); 129.9, 127.8, 126.8 (Ph); 122.0 (CN); 89.2, 86.8 (Cp); 84.4 (C_β); 67.9 (C_α); 60.5 (CH_2Ph); 45.9 (NMe); 3.1 (SiMe₃). A ^{13}C-enriched sample was obtained by using a solution of K^{13}CN (5.0 mg, 0.075 mmol) and NBu$_4^n$CN (200 mg, 0.75 mmol) in CH₃CN/MeOH (3 + 3 mL). IR (CH₂Cl₂) ν(^{13}CN) 2139 (m), ν(CO) 1972 (vs), 1786 (s) cm^{-1}. $^{13}C\{^1H\}$ NMR (CDCl₃) δ 237.29 (μ-CO); 200.5 (CO); 176.6 (d, $^3J_{CC}$ = 5.1 Hz, C_γ); 137.9 (ipso-Ph); 129.9, 127.8, 126.8 (Ph); 121.9 (CN); 89.2, 86.8 (Cp); 84.4 (d, $^2J_{CC}$ = 5.1 Hz, C_β); 67.9 (d, $^1J_{CC}$ = 63.3 Hz, C_α); 60.4 (CH_2Ph); 45.9 (NMe); 3.0 (SiMe₃).

4.9. Synthesis of $[Fe_2\{\mu\text{-}\eta^1\text{:}\eta^3\text{-}C_\gamma(R')C_\beta(R')C_\alpha$ $(CN)N(Me)(R)\}(\mu\text{-}CO)(CO)(Cp)_2]$ (R = Me, R' = Me (9a); R = Me, R' = Ph (9b); R = CH$_2$Ph, R' = Me (9c); R = CH$_2$Ph, R' = COOMe (9d))

A solution of **2a** (90 mg, 0.162 mmol), in CH₂Cl₂ (10 mL), was treated at room temperature with NBu$_4^n$CN (68 mg, 0.254 mmol). The mixture was stirred for 20 min, then it was filtered on alumina. Solvent removal, under reduced pressure, gave **2a** as microcrystalline powder. Yield: 64 mg (91%). Crystals suitable for X-ray analysis were collected by layering a diethyl ether solution of **9a** with petroleum ether (b.p. 40–60 °C), at −20 °C. Anal. Calc. for $C_{20}H_{22}Fe_2N_2O_2$: C, 55.34; H, 5.11; N, 6.45. Found: C, 55.39; H, 5.08; N, 6.49%. IR (CH₂Cl₂) ν(C≡N) 2184 (m), ν(CO) 1956 (vs), 1781 (s) cm^{-1}. ^1H NMR (CDCl₃) 4.85, 4.38 (s, 10H, Cp); 3.80 (s, 3H, C_γMe); 2.22 (s, 3H, C_βMe); 2.12, 1.60 (s, 6H, NMe). $^{13}C\{^1H\}$ NMR (CDCl₃) δ 268.3 (μ-CO); 213.3 (CO); 195.1 (C_γ); 120.0 (CN); 88.9, 86.7 (Cp); 89.1 (C_β); 64.0 (C_α); 48.1, 41.2 (NMe); 39.3 ($C_\gamma Me$); 22.3 ($C_\beta Me$).

Complexes **9b**–**9d** were prepared by the same procedure described for **9a**, by reacting NBu$_4^n$CN with **2b**–**d**, respectively.

9b: Yield (85%). Anal. Calc. for $C_{30}H_{26}Fe_2N_2O_2$: C, 64.55; H, 4.69; N, 5.02. Found: C, 64.63; H, 4.74; N, 5.10%. IR (CH₂Cl₂) ν(C≡N) 2187 (m), ν(CO) 1968 (vs), 1788 (s) cm^{-1}. ^1H NMR (CD₂Cl₂) 7.96–6.63 (m, 10H, Ph); 4.76, 4.53 (s, 10H, Cp); 2.38, 2.03 (s, 6H, NMe). $^{13}C\{^1H\}$ NMR (CD₂Cl₂) δ 265.3 (μ-CO); 214.1 (CO); 197.9 (C_γ); 158.3, 140.7, 133.2, 129.0, 128.3, 128.1, 127.6, 127.2, 124.7 (Ph); 120.1 (CN); 96.5 (C_β); 91.3, 87.9 (Cp); 63.3 (C_α); 50.3, 43.1 (NMe).

9c: Yield (77%). Anal. Calc. for $C_{26}H_{26}Fe_2N_2O_2$: C, 61.21; H, 5.14; N, 5.49. Found: C, 61.15; H, 5.16; N, 5.50%. IR (CH₂Cl₂) ν(C≡N) 2183 (m), ν(CO) 1965 (vs), 1779 (s) cm^{-1}. ^1H NMR (CDCl₃) 7.27–7.04 (m, 5H, Ph); 4.93, *4.89*, 4.44, *4.35* (s, 10H, Cp); 3.87, *3.76* (s, 3H, C_γMe); 4.43, 3.10, *3.04*, 2.94 (d, 2H, $^2J_{HH}$ = 12 Hz, CH_2Ph); 2.26, *2.21* (s, 3H, C_βMe); *2.08*, 1.51 (s, 3H, NMe); Isomer ratio 6:5. $^{13}C\{^1H\}$ NMR (CDCl₃) δ 269.1, 267.4 (μ-CO); 214.2, *212.7* (CO); 196.5, *195.5* (C_γ); 137.7–126.7 (Ph); 120.3 (CN); *89.2*, 89.0, *87.2*, 87.0 (Cp); *90.4*, 88.4 (C_β); 65.2, *64.6* (C_α); 59.5 (CH_2Ph); 45.1, *39.4* (NMe); 38.7 ($C_\gamma Me$); *23.3*, 22.5 ($C_\beta Me$).

9d: Yield: (80%). Anal. Calc. for $C_{28}H_{26}Fe_2N_2O_6$: C, 56.22; H, 4.38; N, 4.68. Found: C, 56.30; H, 4.27; N, 4.72%. IR (CH₂Cl₂) ν(C≡N) 2191 (w), ν(CO) 1987 (vs), 1801 (s), 1720 (m) cm^{-1}. ^1H NMR (CDCl₃) 7.36–7.19 (m, 5H, Ph); 4.93, *4.89*, 4.79, *4.70* (s, 10H, Cp); 4.35, *3.74*, 3.64, 3.21 (d, 2H, $^2J_{HH}$ = 12 Hz, CH_2Ph); *4.04*, 4.01, *3.91*, 3.87 (s, 6H, CO₂Me); *2.07*, 1.67 (s, 3H, NMe); Isomer ratio 3:1. $^{13}C\{^1H\}$ NMR (CDCl₃) δ 260.2 (μ-CO); *211.8*, 210.2 (CO); *186.0*, 184.7, 179.1, 170.8 (C_γ and CO₂Me); 136.9–127.0 (Ph); *119.4*, 119.2 (CN); *89.5*, 89.2, *89.0*, 88.6 (Cp); 88.1 (C_β); *65.3*, 59.2 (CH_2Ph); 62.9 (C_α); 53.2, *52.9*, 52.4, *52.2* (CO₂Me); 45.4, *36.9* (NMe).

4.10. Synthesis of $[Fe_2\{\mu\text{-}\eta^1\text{:}\eta^2\text{-}C_\gamma(CO_2Me)C_\beta(CO_2Me)(CN)C_\alpha N(Me)(Xyl)\}(\mu\text{-}CO)(CO)(Cp)_2]$ (10)

A solution of **2e** (98 mg, 0.133 mmol), in CH₂Cl₂ (10 mL), was treated at room temperature with NBu$_4^n$CN (43 mg, 0.160 mmol). After 30 min of stirring, the solvent was removed under reduced pressure. Chromatography on alumina, with CH₂Cl₂ as eluent, afforded **10** as a brown band. Yield: 59 mg (71%). Anal. Calc. for $C_{29}H_{28}Fe_2N_2O_6$: C, 56.89; H, 4.61; N, 4.58. Found: C, 56.77; H, 4.62; N, 4.53%. IR (CH₂Cl₂) ν(C≡N) 2175 (w), ν(CO) 1947 (vs), 1777 (s), 1733 (m), 1683 (m) cm^{-1}. ^1H NMR (CDCl₃) 7.33–7.14 (m, 3H, Me₂C_6H_3); 4.69, 4.19 (s, 10H, Cp); 3.95, 3.91 (s, 6H, CO₂Me); 3.36 (s, 3H, NMe); 2.15, 2.12 (s, 6H, Me₂C_6H_3). $^{13}C\{^1H\}$ NMR (CDCl₃) δ 272.3 (μ-CO); 252.7 (C_α); 214.6 (CO); 182.3 (C_γ-CO₂Me); 168.5 (C_β-CO₂Me); 145.2 (ipso-Me₂C_6H_3); 134.1, 132.8, 129.7, 128.6, 128.3 (Me₂C_6H_3); 129.4 (C_γ); 116.5 (C_βCN); 88.3, 87.6 (Cp); 81.5 (C_β); 53.5, 50.9 (CO₂Me); 44.9 (NMe); 18.1, 17.5 (Me₂C_6H_3). A ^{13}C-enriched sample on the CN

position was obtained by using a solution of $K^{13}CN$ (5.0 mg, 0.075 mmol) and $NBu_4^n CN$ (200 mg, 0.75 mmol) in CH_3CN (6 mL). IR (CH_2Cl_2) $v(^{13}C\equiv N)$ 2090 (m), $v(CO)$ 1947 (vs), 1777 (s), 1733 (m), 1683 (m) cm^{-1}. $^{13}C\{^1H\}$ NMR (CDCl$_3$) δ 272.7 (μ-CO); 253.0 (C$_\alpha$); 214.8 (CO); 182.5 (C$_\gamma$-CO_2Me); 168.7 (C$_\beta$-CO_2Me); 145.3 (ipso-Me$_2$C$_6$H$_3$); 134.2, 133.0, 129.8, 128.7, 128.4 (Me$_2$C$_6$H$_3$); 129.4 (d, $^2J_{CC}$ = 5.0 Hz, C$_\gamma$); 116.6 (C$_\beta$CN); 88.3, 87.6 (Cp); 81.5 (d, $^1J_{CC}$ = 67.2 Hz, C$_\beta$); 53.5, 50.9 (CO$_2$Me); 44.8 (NMe); 18.0, 17.4 (Me$_2$C$_6$H$_3$).

4.11. X-ray crystallography for 3a and 9a

The diffraction experiments were carried out at room temperature on a Bruker AXS SMART 2000 CCD based diffractometer using graphite monochromated Mo Kα radiation ($\lambda = 0.71073$ Å). Intensity data were measured over full diffraction sphere using 0.3° wide ω scans. The software SMART [11] was used for collecting frames of data, indexing reflections and determination of lattice parameters. The collected frames were then processed for integration by software SAINT [11] and an empirical absorption correction was applied with SADABS [12]. The structures were solved by direct methods (SIR97) [13] and subsequent Fourier syntheses, and refined by full-matrix least-squares calculations on F^2 (SHELXTL) [14] attributing anisotropic

thermal parameters to all the non-hydrogen atoms. In complex 3a, the Cp ligand bound to Fe(1) was disordered over two positions and the site occupation factors were refined yielding the values 0.60 and 0.40, respectively whereas in complex 9a both Cp ligands were disordered over two positions and their site occupation factors were refined yielding the values 0.73 and 0.27 for the Cp bound to Fe(1) [0.64 and 0.36, respectively, for the Cp bound to Fe(2)]. The methyl and aromatic hydrogen atoms were placed in calculated positions and refined with idealized geometry, whereas the H atom bound to C(4) in 3a was located in the Fourier map and refined isotropically. In order to be sure about the mode of bonding of 3a and 9a, structure models of alternative assignments of the carbon and nitrogen positions were refined (cyanide, isocyanide). The isocyanide models for the independent molecules in 3a and 9a showed worsening of the agreement indices and physically unreasonable thermal motion ellipsoids (see Table 2).

Appendix A. Supplementary material

Crystallographic data for the structures reported in this paper have been deposited with the Cambridge Crystallographic Data Centre as supplementary publication nos. CCDC 608048 and CCDC 608049 for 3a and 9a, respectively. Copies of the data can be obtained free of charge on application to CCDC, 12 Union Road, Cambridge CB21EZ, UK, fax: +44 1223 336 033, e-mail: deposit@ ccdc.cam.ac.uk.

Table 2
Crystal data and experimental details for **3a** and **9a**

Compound	3a	9a
Formula	C$_{21}$H$_{26}$Fe$_2$N$_2$O$_2$Si	C$_{20}$H$_{22}$Fe$_2$N$_2$O$_2$
Fw	478.23	434.10
T (K)	293(2)	293(2)
λ (Å)	0.71073	0.71073
Crystal symmetry	monoclinic	monoclinic
Space group	$P2_1/n$	$P2_1/n$
Unit cell dimensions		
a (Å)	10.5739(3)	7.9451(3)
b (Å)	28.4979(8)	16.3339(7)
c (Å)	15.2823(4)	14.3416(6)
α (°)	90	90
β (°)	109.319(1)	99.369(1)
γ (°)	90	90
Cell volume (Å^3)	4345.8(2)	1836.4(1)
Z	8	4
D_{calc} (Mg m^{-3})	1.462	1.570
μ(Mo K$_\alpha$) (mm^{-1})	1.409	1.596
$F(000)$	1984	896
Crystal size (mm)	0.35 × 0.30 × 0.28	0.30 × 0.28 × 0.25
θ Limits (°)	1.43–30.02	1.90–30.03
Reflections collected	56753($\pm h, \pm k, \pm l$)	23289($\pm h, \pm k, \pm l$)
Unique observed reflections		
[$F_o > 4\sigma(F_o)$] (R_{int})	12692 (0.0652)	5364 (0.0264)
Goodness-of-fit-on F^2	0.934	1.034
R_1 (F)[a], wR_2 (F^2)[b]	0.0419, 0.0964	0.0286, 0.0772
Largest difference in peak and hole (e Å^{-3})	0.504/−0.471	0.270/−0.485

[a] $R_1 = \sum ||F_o| - |F_c||/\sum |F_o|$.

[b] $wR_2 = \left[\sum w(F_o^2 - F_c^2)^2 / \sum w(F_o^2)^2 \right]_{1/2}$, where $w = 1/[\sigma^2(F_o^2) + (aP)^2 + bP]$, where $P = (F_o^2 + 2F_c^2)/3$.

References

[1] (a) R.A. Adams, F.A. Cotton (Eds.), Catalysis by Di-and Polynuclear Metal Complexes, Wiley–VCH, New York, 1998;
(b) P. Braunstein, J. Rosè, in: P. Braunstein, L.A. Oro, P.R. Raithby (Eds.), Metal Cluster in Chemistry, Wiley–VCH, Weinheim, 1999, p. 616;
(c) M.V. Jimenéz, E. Sola, F.J. Lahoz, L.A. Oro, Organometallics 24 (2005) 2722;
(d) R.D. Adams, B. Captain, J. Organomet. Chem. 689 (2004) 4521;
(e) B. Bosnich, Inorg. Chem. 38 (1999) 2554;
(f) B.D. Rowsell, R. McDonald, M. Cowie, Organometallics 23 (2004) 3873.
[2] (a) V.G. Albano, L. Busetto, F. Marchetti, M. Monari, S. Zacchini, V. Zanotti, Organometallics 22 (2003) 1326;
(b) V.G. Albano, L. Busetto, F. Marchetti, M. Monari, S. Zacchini, V. Zanotti, J. Organomet. Chem. 689 (2004) 528.
[3] (a) V.G. Albano, L. Busetto, F. Marchetti, M. Monari, S. Zacchini, V. Zanotti, Organometallics 23 (2004) 3348;
(b) V.G. Albano, L. Busetto, F. Marchetti, M. Monari, S. Zacchini, V. Zanotti, J. Organomet. Chem. 690 (2005) 837.

[4] L. Busetto, F. Marchetti, S. Zacchini, V. Zanotti, Organometallics 24 (2005) 2297.

[5] V.G. Albano, L. Busetto, F. Marchetti, M. Monari, S. Zacchini, V. Zanotti, J. Organomet. Chem. 690 (2005) 4666.

[6] L. Busetto, F. Marchetti, S. Zacchini, V. Zanotti, J. Organomet. Chem. 691 (2006) 2424.

[7] R.B. King, Coordin. Chem. Rev. 248 (2004) 1533.

[8] (a) V. Zanotti, S. Bordoni, L. Busetto, L. Carlucci, A. Palazzi, R. Serra, V.G. Albano, M. Monari, F. Prestopino, F. Laschi, P. Zanello, Organometallics 14 (1995) 5232;
(b) L. Busetto, V. Zanotti, J. Organomet. Chem. 690 (2005) 5430.

[9] W. Wilker, D. Leibfritz, R. Kerssebaum, W. Beimel, Magn. Reson. Chem. 31 (1993) 287.

[10] K. Stott, J. Stonehouse, J. Keeler, T.L. Hwang, A.J. Shaka, J. Am. Chem. Soc. 117 (1995) 4199.

[11] SMART & SAINT Software Reference Manuals, Version 5.051 (Windows NT Version), Bruker Analytical X-ray Instruments Inc., Madison, WI, 1998.

[12] G.M. Sheldrick, SADABS, Program for Empirical Absorption Correction, University of Göttingen, Germany, 1996.

[13] A. Altomare, M.C. Burla, M. Cavalli, G.L. Cascarano, C. Giacovazzo, A. Guagliardi, A.G.G. Moliterni, G. Polidori, R. Spagna, J. Appl. Cryst. 32 (1999) 115.

[14] G.M. Sheldrick, SHELXTLplus Version 5.1 (Windows NT Version) Structure Determination Package, Bruker Analytical X-ray Instruments Inc., Madison, WI, 1998.